

# Electronic Supplementary Material

## **Petroleum pitch derived hard carbon via NaCl-template as anode materials with high rate performance for sodium ion battery**

Baoyu Wu<sup>1</sup>, Hao Sun<sup>1</sup>, Xiaoxue Li<sup>1</sup>, Yinyi Gao<sup>1</sup>, Tianzeng Bao<sup>2</sup>, Hongbin Wu<sup>2</sup>, Kai Zhu (✉)<sup>1</sup>, Dianxue Cao (✉)<sup>1</sup>

1 Key Laboratory of Superlight Materials and Surface Technology of Ministry of Education, College of Materials Science and Chemical Engineering, Harbin Engineering University, Harbin 150001, China

2 Hunan Hongshan New Energy Technology Co., Ltd, Yiyang City 413000, China

E-mails: [kzhu@hrbeu.edu.cn](mailto:kzhu@hrbeu.edu.cn) (Zhu K); [caodianxue@hrbeu.edu.cn](mailto:caodianxue@hrbeu.edu.cn) (Cao D)

Contents:

TGA.

SEM and HRTEM images.

TEM images.

Nitrogen uptake and desorption curve and pore size distribution curve.

XPS C1s spectra.

The first three laps Static charge/discharge curves.

the cycling performance of materials prepared with varying NaCl ratios at 0.5A g<sup>-1</sup>.

The CVs at different scanning rates.

The CVs curve for the first three cycles of HC materials at a scan rate of 0.2mV/s.

Log-Log plot.

The ex-situ TEM images.

The measurements of specific surface area and pore size were made on various materials.

Table of the area of the different peaks of the XPS and their ratios.

The comparison of electrochemical properties with other reported data.

Table of the Resistance values to fit EIS.

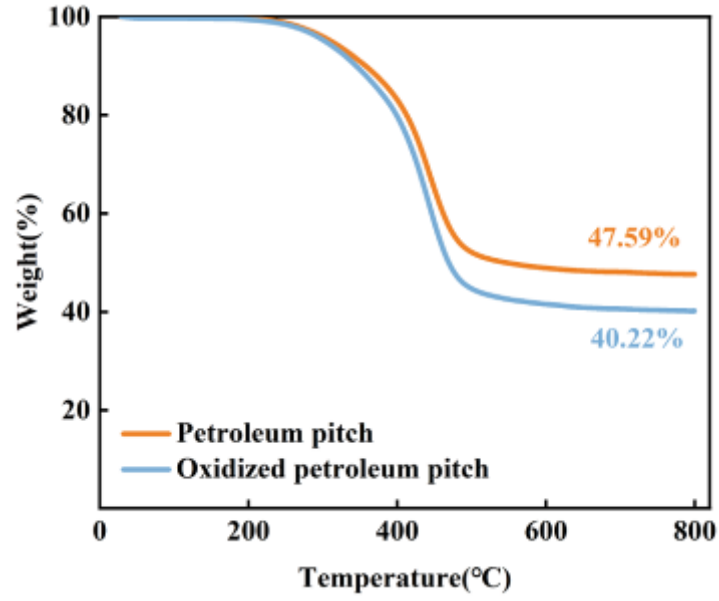


Fig. S1 The TGA curves of petroleum pitch and oxidized petroleum pitch.

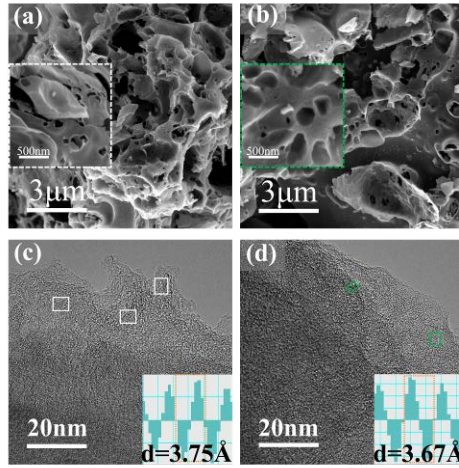


Fig. S2 (a) The SEM image of HC1500-8 and its enlarged image. (b) The SEM image of HC1300-10 and its enlarged image. (c) The HRTEM image of HC1500-8. (d) The HRTEM image of HC1500-12.

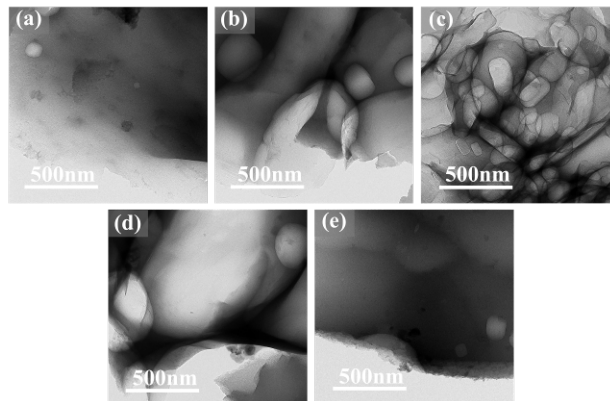


Fig. S3 (a) The TEM image of HC1100-10. (b) The TEM image of HC13300-10. (c) The TEM image of HC1100-10. (d) The HRTEM image of HC1500-8. (e) The HRTEM image of HC1500-12.

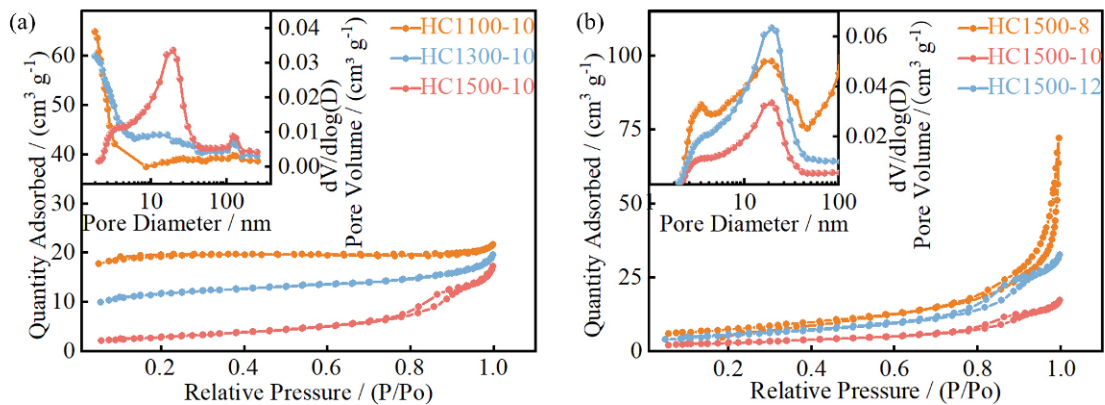


Fig. S4 (a) Nitrogen uptake and desorption curve and pore size distribution curve of HC at various carbonization temperatures. (b) Nitrogen uptake and desorption curve and pore size distribution curve of HC at various carbonization times.

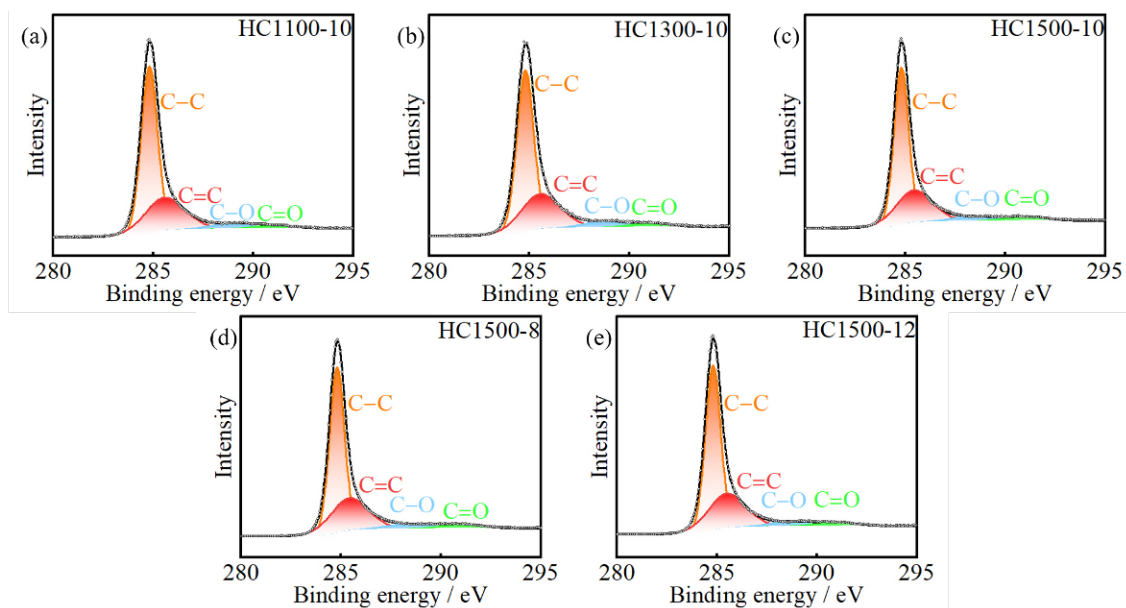


Fig. S5 (a) XPS C1s spectra of the HC1100-10. (b) XPS C1s spectra of the HC1300-10. (c) XPS C1s spectra of the HC1500-10. (d) XPS C1s spectra of the HC1500-8. (e) XPS C1s spectra of the HC1500-12.

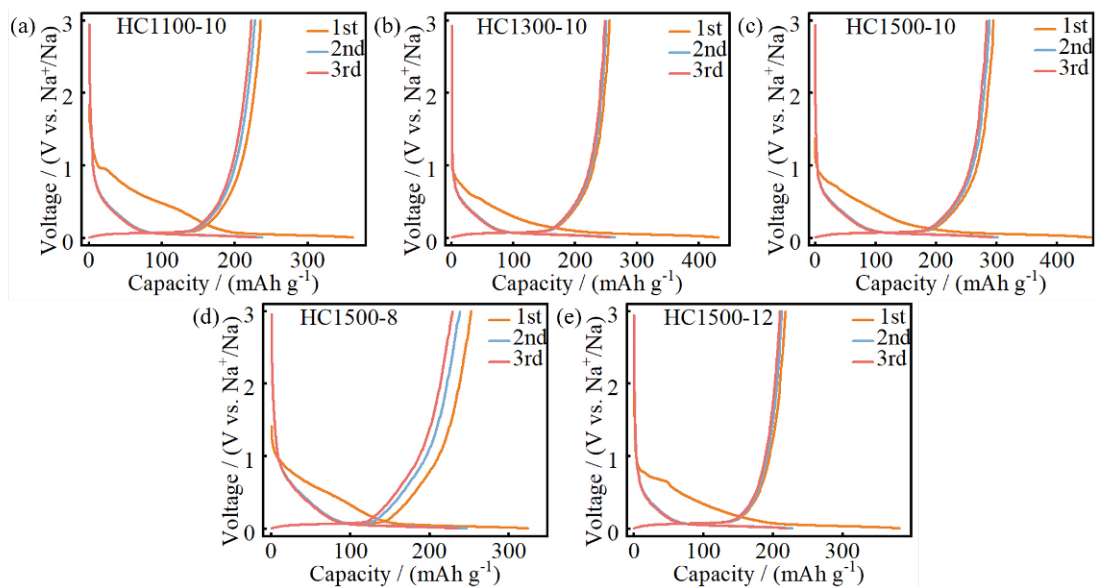


Fig. S6. (a) The first three laps Static charge/discharge curves of HC1100-10 at  $0.1 \text{ A g}^{-1}$ . (b) The first three laps Static charge/discharge curves of HC1300-10 at  $0.1 \text{ A g}^{-1}$ . (c) The first three laps Static charge/discharge curves of HC1500-10 at  $0.1 \text{ A g}^{-1}$ . (d) The first three laps Static charge/discharge curves of HC1500-8 at  $0.1 \text{ A g}^{-1}$ . (e) The first three laps Static charge/discharge curves of HC1500-12 at  $0.1 \text{ A g}^{-1}$ .

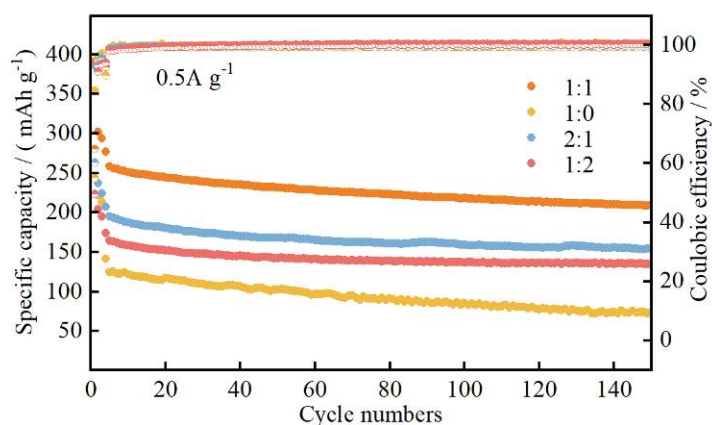


Fig. S7 The cycling performance of materials prepared with varying NaCl ratios at  $0.5 \text{ A g}^{-1}$ .

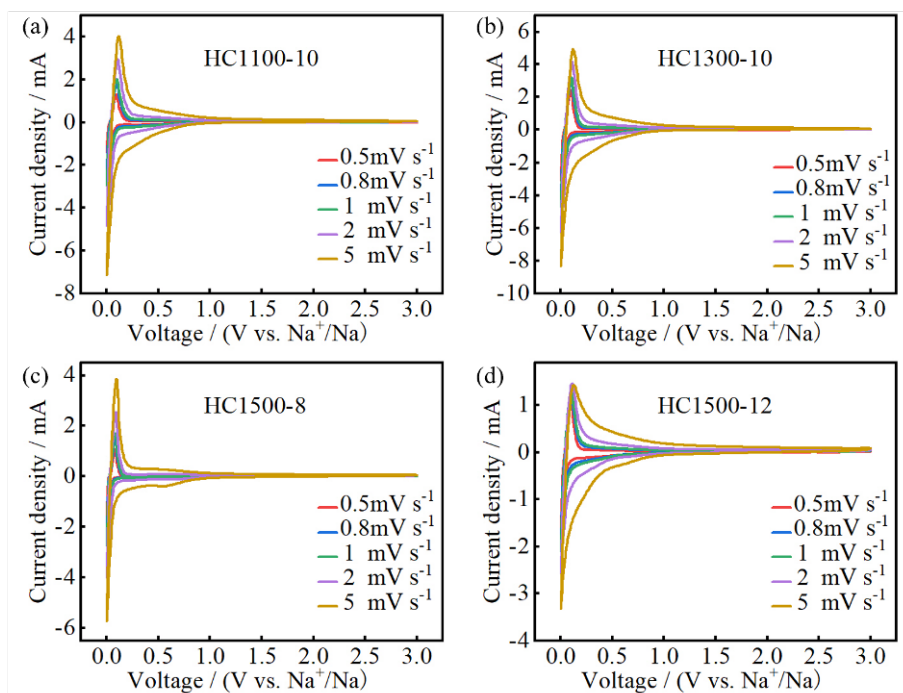


Fig. S8 (a) The CVs of HC1100-10 at different scanning rates. (b) The CVs of HC1300-10 at different scanning rates. (c) The CVs of HC1500-8 at different scanning rates. (d) The CVs of HC1500-12 at different scanning rates.

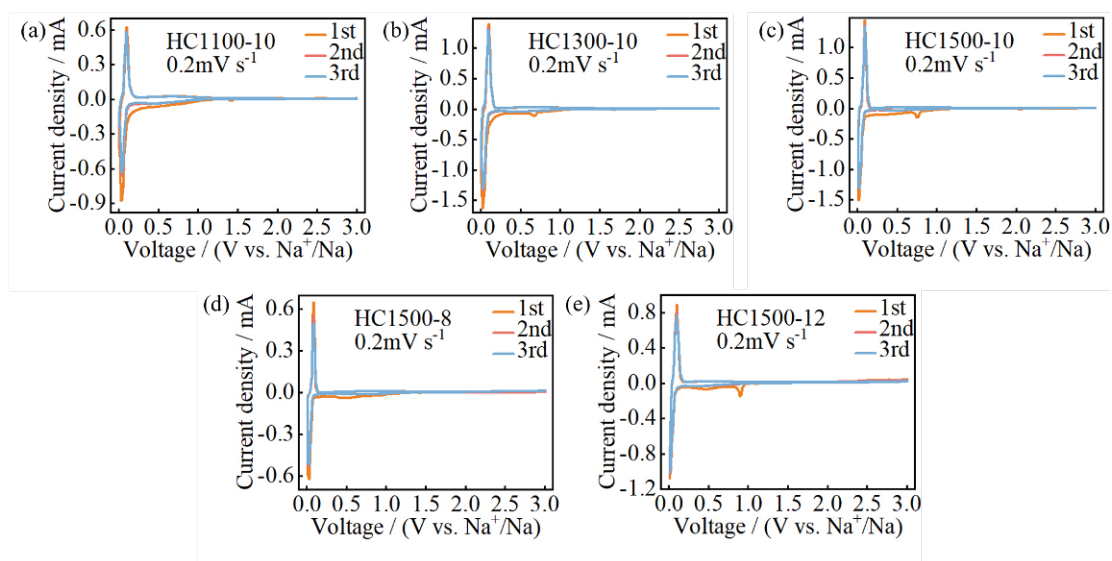


Fig. S9 (a) The CV curves of HC1100-10 at a scan rate of 0.2mV/s. (b) The CV curves of HC1300-10 at a scan rate of 0.2mV/s. (c) The CV curves of HC1500-10 at a scan rate of 0.2mV/s. (d) The CV curves of HC1500-8 at a scan rate of 0.2mV/s. (e) The CV curves of HC1500-12 at a scan rate of 0.2mV/s.

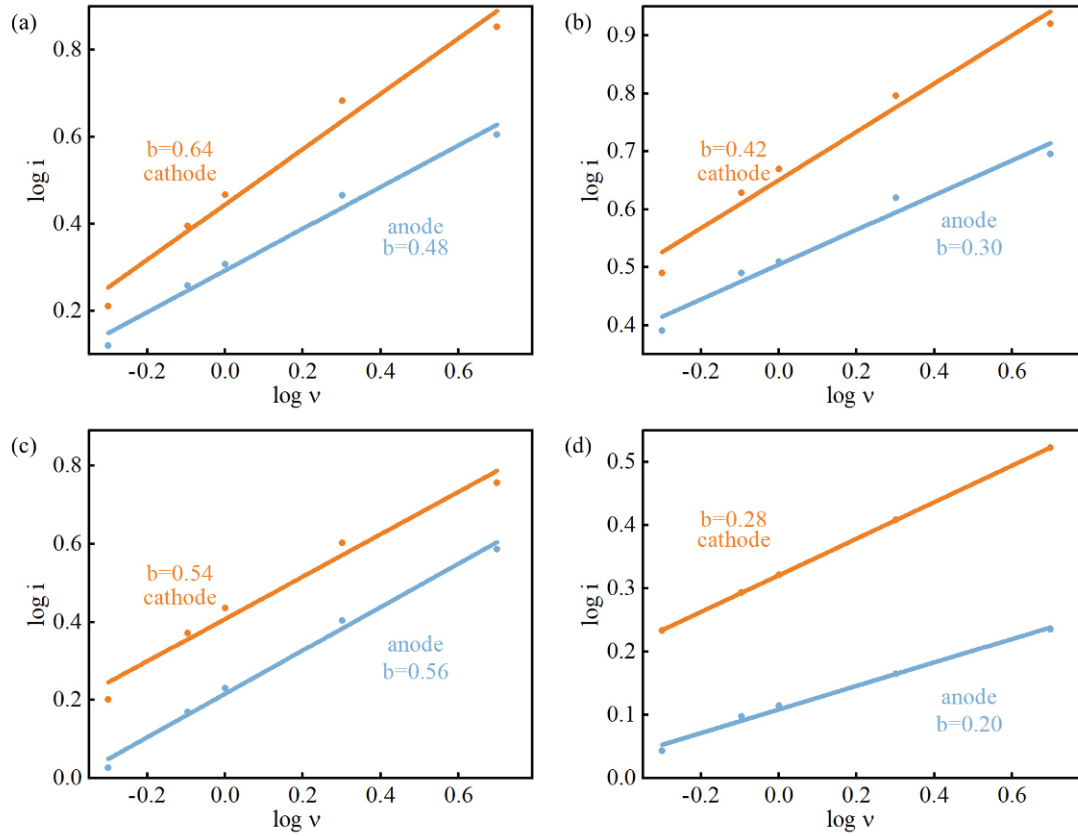


Fig. S10 (a) The b-value of cathode and anode peaks by Log(peak current)-Log(scanning rate) plot of HC1100-10. (b) The b-value of cathode and anode peaks by Log(peak current)-Log(scanning rate) plot of HC1300-10. (c) The b-value of cathode and anode peaks by Log(peak current)-Log(scanning rate) plot of HC1500-8. (d) The b-value of cathode and anode peaks by Log(peak current)-Log(scanning rate) plot of HC1500-12.

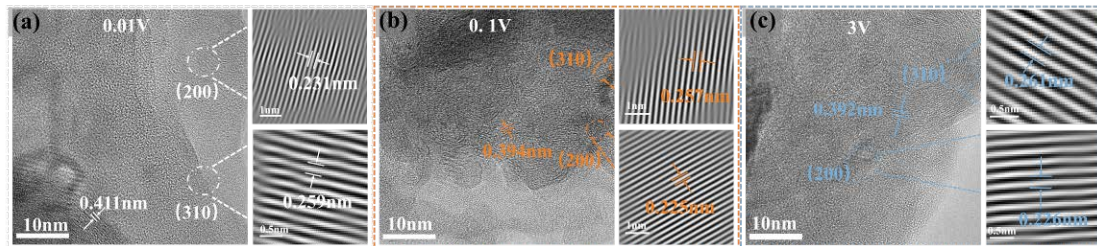


Fig. S11 The ex-situ TEM images were taken at various voltages.

Table S1 The measurements of specific surface area and pore size were made on various materials.

The name of the material	The specific surface area	The average pore diameter
HC1100-10	59.1151 m <sup>2</sup> g <sup>-1</sup>	4.1203 nm
HC1300-10	37.4629 m <sup>2</sup> g <sup>-1</sup>	5.4734 nm
HC1500-10	10.4899 m <sup>2</sup> g <sup>-1</sup>	10.5746 nm
HC1500-8	26.7083 m <sup>2</sup> g <sup>-1</sup>	12.0789 nm
HC1500-12	19.6106 m <sup>2</sup> g <sup>-1</sup>	10.5047 nm
OPP1500-10	1.7566 m <sup>2</sup> g <sup>-1</sup>	7.5121 nm

Table S2 The  $sp^2$  peak, the  $sp^3$  peak and their area ratios in XPS of different HC materials

The name of the material	Peak area about $sp^2$	Peak area about $sp^3$	Peak area about $sp^2$ / Peak area about $sp^3$
HC1100-10	51031.94	101753	0.501527621
HC1300-10	49875.62	94758.52	0.526344438
HC1500-10	58453.83	110391.85	0.529512188
HC1500-8	100553.73	194434.72	0.517159332
HC1500-12	98828.96	183528.72	0.538493158

Table S3 The comparison of electrochemical properties with other reported data.

Methods and materials	Specific capacity	Current density	Carbonization temperature and time	Ref
coal-based carbons coated by pitch-derived soft carbon	188.2 mA g <sup>-1</sup>	0.5 A g <sup>-1</sup>	1200°C 2h	1
Petroleum asphalt oxidized with HNO <sub>3</sub>	226.8 mA g <sup>-1</sup>	0.3 A g <sup>-1</sup>	1300°C 3h	2
Pre-oxidized coal tar pitches.	Around 150 mA g <sup>-1</sup>	0.3 A g <sup>-1</sup>	1200°C 2h	3
Mn microregulated pitch	230 mA g <sup>-1</sup>	0.5 A g <sup>-1</sup>	800°C 2h	4
petroleum pitch as the carbon source and NaCl as template	276.59 mA g <sup>-1</sup>	0.5 A g <sup>-1</sup>	1500°C 10h	This work

Table S4 The Resistance values of different HC materials to fit EIS

The name of the material	Rs	Rct
HC1100-10	2.851	22.69
HC1300-10	2.882	32.26
HC1500-8	2.773	22.47
HC1500-10	2.686	15.49
HC1500-12	8.697	20.21

## References

- Chen H, Sun N, Wang Y X, Soomro R A and Xu B. One stone two birds: Pitch assisted microcrystalline regulation and defect engineering in coal-based carbon anodes for sodium-ion batteries. *Energy Storage Materials*. 2023, 56: 532-541
- Xiong Z Y, Yue L, Zhang Y, Ding H F, Bai L X, Zhao Q, Mei T H, Cao J, Qi Y R and Xu M W. Structural

regulation of asphalt-based hard carbon microcrystals based on liquid-phase crosslinking to enhance sodium storage. *Journal of Colloid and Interface Science*. 2024, 658: 610-616

3. Ji L C, Zhao Y, Cao L J, Li Y, Ma C L, Qi X G and Shao Z P. A fundamental understanding of structure evolution in the synthesis of hard carbon from coal tar pitch for high-performance sodium storage. *Journal of Materials Chemistry A*. 2023, 11(48): 26727-26741

4. Shao Y, Yang Q, Zhang Y, Jiang N, Hao Y H, Qu K Q, Du Y D, Qi J, Li Y, Tang Y C, et al. A Universal Method for Regulating Carbon Microcrystalline Structure for High-Capacity Sodium Storage: Binding Energy As Descriptor. *ACS Nano*. 2023, 17(23): 24012-24021